

Josephson effect and spin-triplet pairing correlations in SF_1F_2S junctions

Luka Trifunovic,* Zorica Popović, and Zoran Radović

Department of Physics, University of Belgrade, P.O. Box 368, 11001 Belgrade, Serbia

We study theoretically the Josephson effect and pairing correlations in planar SF_1F_2S junctions that consist of conventional superconductors (S) connected by two metallic monodomain ferromagnets (F_1 and F_2) with transparent interfaces. We obtain both spin-singlet and -triplet pair amplitudes and the Josephson current-phase relations for arbitrary orientation of the magnetizations using the self-consistent solutions of Eilenberger equations in the clean limit and for a moderate disorder in ferromagnets. We find that the long-range spin-triplet correlations cannot prevail in symmetric junctions with equal ferromagnetic layers. Surprisingly, the long-range spin-triplet correlations give the dominant second harmonic in the Josephson current-phase relation of highly asymmetric SF_1F_2S junctions. The effect is robust against moderate disorder and variations in the layers thickness and exchange energy of ferromagnets.

PACS numbers: 74.45.+c, 74.50.+r

I. INTRODUCTION

Spin-triplet superconducting correlations induced in heterostructures comprised of superconductors with the usual spin-singlet pairing and inhomogeneous ferromagnets have attracted considerable attention recently.¹ Triplet pairing which is odd in frequency was envisaged a long ago² in an attempt to describe the A phase of superfluid ^3He . Even though it was found that the pairing in superfluid ^3He is odd in space (p-wave) rather than in time, it is predicted that even in space (s-wave) and odd in time (odd in frequency) pairing does occur in certain superconductor (S) – ferromagnet (F) structures with inhomogeneous magnetization.^{3,4} As a result, superconducting correlations can have a long-range propagation from SF interfaces, with penetration lengths up to $1\mu\text{m}$ and a nonvanishing Josephson supercurrent through very strong ferromagnets.^{5–11}

The first evidence of long-range S–F proximity effect came from the experiments on long wires made of Ho conical ferromagnet,⁵ and a fully-spin-polarized CrO_2 halfmetallic ferromagnet,⁶ in which Josephson supercurrent was measured. These experimental findings were subsequently verified using different substrates and superconducting contacts.⁷ Very recently, the effect has also been observed in single-crystal ferromagnetic Co nanowires,⁸ a Heusler alloy Cu_2MnAl ,⁹ and synthetic antiferromagnets with no net magnetization where thin PdNi or Ho layers are combined with Co layers.^{10,11}

In SFS Josephson junctions with homogeneous¹² or spiral¹³ magnetization, the projection of the total spin of a pair to the direction of magnetization is conserved and only spin-singlet f_s and triplet f_{t0} correlations with zero spin projection occur. These correlations penetrate into the ferromagnet over a short distance determined by the exchange energy. For inhomogeneous magnetization, odd-frequency triplet correlations f_{t1} with nonzero (± 1) total spin projection are present as well. These correlations, not suppressed by the exchange interaction, are long-ranged and have a dramatic impact on transport properties and the Josephson effect.¹

Dominant influence of long-range triplet correlations on the Josephson current can be realized in SFS junctions with magnetically active interfaces,^{14,15} narrow domain walls between S and thick F interlayers with misaligned magnetizations,^{16–21} or superconductors with spin orbit interaction.²² In general, fully developed triplet proximity effect can be realized only after inserting a singlet-to-triplet “converter,” a thin (weak) ferromagnetic layer sandwiched between a superconductor and a thick (strong) ferromagnet, acting as a “filter” which suppresses the short-range correlations.^{16–20}

The simplest superconductor-ferromagnet heterostructures with inhomogeneous magnetization are F_1SF_2 and SF_1F_2S junctions with monodomain ferromagnetic layers having noncollinear in-plane magnetizations. These structures have been studied using Bogoliubov-de Gennes equation^{23–26} and within the quasiclassical approximation in diffusive^{27–34} and clean^{35,36} limits using Usadel and Eilenberger equations, respectively. It has been expected that the critical supercurrent in SF_1F_2S junctions has a nonmonotonic dependence on angle between magnetizations due to the long-ranged spin-triplet correlations. However, in symmetric junctions a monotonic dependence has been found both in the clean and dirty limits, except for nonmonotonicity caused by $0 - \pi$ transitions.^{23,32}

Apparently, the long-range Josephson effect is not feasible in the junctions with only two F layers,^{17,19} except in highly asymmetric SF_1F_2S junctions at low temperatures, as we will show here. In this case, the long-range spin-triplet effect manifests itself as a large second harmonic ($I_2 \gg I_1$) in the spectral decomposition of the Josephson current-phase relation, $I(\phi) = I_1 \sin(\phi) + I_2 \sin(2\phi) + \dots$. The ground state in Josephson junctions with ferromagnet can be 0 or π state.¹² The energy of the junction is proportional to $\int_0^\phi I(\phi') d\phi'$, hence a second harmonic leads to degenerate ground states at $\phi = 0$ and $\phi = \pi$. Small contribution of the first harmonic lifts the degeneracy which results in coexistence of stable and metastable 0 and π states.³⁷

In this article, we study the Josephson effect and influ-

ence of odd-frequency spin-triplet superconducting correlations in clean and moderately disordered SF_1F_2S junctions with transparent interfaces. Magnetic interlayer is composed of two monodomain ferromagnets with arbitrary orientation of in-plane magnetizations. We calculate pair amplitudes and the Josephson current from the self-consistent solutions of the Eilenberger equations. Pair amplitudes f_s and f_{t0} are short-ranged, while f_{t1} is long-ranged.

We show that the influence of misalignment of magnetizations on the Josephson current in symmetric SFFS junctions with equal ferromagnetic layers cannot be attributed to the emergence of long-range spin-triplet correlations: For thin F layers (compared to the ferromagnetic exchange length) all pair amplitudes are equally large, while for thick F layers the long-range triplet component is very small. This explains why no substantial impact of long-range spin-triplet superconducting correlations on the Josephson current has been found previously for symmetric SFFS junctions both in the ballistic and diffusive regimes.^{23,32}

We find that long-range spin-triplet Josephson current can be realized only in highly asymmetric SF_1F_2S junctions composed of particularly thin (weak) and thick (strong) ferromagnetic layers with noncollinear magnetizations at low temperatures. In that case the second harmonic in the Josephson current-phase relation is dominant.

The dominant second harmonic provides more sensitive quantum interferometers (SQUIDS) with effectively two times smaller flux quantum³⁷ and gives the half-integer Shapiro steps.³⁸ The coexistence of 0 and π ground-state configurations in SQUIDS is potentially useful for experimental study of the quantum superposition of macroscopically distinct states.^{39,40} Particularly asymmetric SF_1F_2S junctions also enable a robust realization of so-called ϕ -junctions.⁴¹ In general, Josephson junctions with a non-sinusoidal current-phase relation are shown to be promising for realization of “silent” phase qubits.^{42,43}

The reminder of the article is organized as follows. In Sec. II, we present the model and the equations that we use to calculate the Josephson current and spin-singlet and triplet pair amplitudes. In Sec. III, we provide numerical results for different ferromagnetic layers thickness and strength and orientation of magnetizations. The conclusion is given in Sec. IV.

II. MODEL AND FORMALISM

We consider a simple model of an SF_1F_2S heterojunction consisting of two conventional (*s*-wave, spin-singlet pairing) superconductors (S) and two uniform monodomain ferromagnetic layers (F_1 and F_2) of thickness d_1 and d_2 , with angle $\alpha = \alpha_2 - \alpha_1$ between their in-plane magnetizations (see Fig. 1). Interfaces between layers are fully transparent and magnetically inactive.

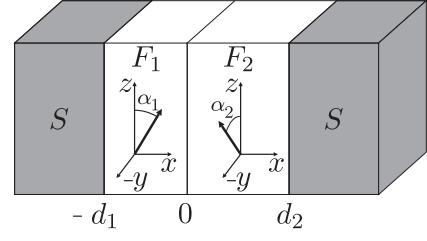


FIG. 1: Schematics of an SF_1F_2S heterojunction. The magnetization vectors lie in the y - z plane at angles α_1 and α_2 with respect to the z -axis.

Superconductivity is described in the framework of the Eilenberger quasiclassical theory.^{1,44} Ferromagnetism is modeled by the Stoner model, using an exchange energy shift $2\hbar$ between the spin subbands. Disorder is characterized by the electron mean free path $l = v_F\tau$, where τ is the average time between scattering on impurities, and v_F is the Fermi velocity assumed to be the same everywhere.

Both the clean and moderately diffusive ferromagnetic layers are considered. In the clean limit, the mean free path l is larger than the two characteristic lengths: the ferromagnetic exchange length $\xi_F = \hbar v_F/\hbar$, and the superconducting coherence length $\xi_S = \hbar v_F/\pi\Delta_0$, where Δ_0 is the bulk superconducting pair potential. For moderate disorder $\xi_F < l < \xi_S$.

In this model, the Eilenberger Green functions $g_{\sigma\sigma'}(x, v_x, \omega_n)$, $g_{\sigma\sigma'}^\dagger(x, v_x, \omega_n)$, $f_{\sigma\sigma'}(x, v_x, \omega_n)$, and $f_{\sigma\sigma'}^\dagger(x, v_x, \omega_n)$ depend on the Cooper pair center-of-mass coordinate x along the junction axis, angle θ of the quasiclassical trajectories with respect to the x axis, projection $v_x = v_F \cos \theta$ of the Fermi velocity vector, and on the Matsubara frequencies $\omega_n = \pi k_B T(2n + 1)$, $n = 0, \pm 1, \dots$. Spin indices are $\sigma = \uparrow, \downarrow$.

The Eilenberger equation in particle-hole \otimes spin space can be written in the compact form

$$\hbar v_x \partial_x \tilde{g} + \left[\omega_n \hat{\tau}_3 \otimes \hat{1} - i\tilde{V} - \tilde{\Delta} + \hbar \langle \tilde{g} \rangle / 2\tau, \tilde{g} \right] = 0, \quad (1)$$

with normalization condition $\tilde{g}^2 = \hat{1}$. We indicate by $\hat{\cdot}$ and $\hat{\cdot} \hat{\cdot}$ 2×2 and 4×4 matrices, respectively. The brackets $\langle \dots \rangle$ denote angular averaging over the Fermi surface (integration over θ), and $[,]$ denotes a commutator. The quasiclassical Green functions

$$\tilde{g} = \begin{bmatrix} g_{\uparrow\uparrow} & g_{\uparrow\downarrow} & f_{\uparrow\uparrow} & f_{\uparrow\downarrow} \\ g_{\downarrow\uparrow} & g_{\downarrow\downarrow} & f_{\downarrow\uparrow} & f_{\downarrow\downarrow} \\ -f_{\uparrow\uparrow}^\dagger & -f_{\uparrow\downarrow}^\dagger & -g_{\uparrow\uparrow} & -g_{\uparrow\downarrow} \\ -f_{\downarrow\uparrow}^\dagger & -f_{\downarrow\downarrow}^\dagger & -g_{\downarrow\uparrow} & -g_{\downarrow\downarrow} \end{bmatrix} \quad (2)$$

are related to the corresponding Gor'kov-Nambu Green functions $\tilde{G} = -i\langle T(\Psi\Psi^\dagger) \rangle$ integrated over energy,

$$\tilde{g} = \frac{i}{\pi} \hat{\tau}_3 \otimes \hat{1} \int d\varepsilon_{\mathbf{k}} \tilde{G}, \quad (3)$$

where $\Psi = (\psi_\uparrow, \psi_\downarrow, \psi_\uparrow^\dagger, \psi_\downarrow^\dagger)^T$ and $\varepsilon_{\mathbf{k}} = \hbar^2 \mathbf{k}^2 / 2m - \mu$. The matrix \tilde{V} is given by

$$\tilde{V} = \hat{1} \otimes \text{Re}[\mathbf{h}(x) \cdot \hat{\boldsymbol{\sigma}}] + i\hat{\tau}_3 \otimes \text{Im}[\mathbf{h}(x) \cdot \hat{\boldsymbol{\sigma}}], \quad (4)$$

where the components $\hat{\sigma}_x, \hat{\sigma}_y, \hat{\sigma}_z$ of the vector $\hat{\boldsymbol{\sigma}}$, and $\hat{\tau}_1, \hat{\tau}_2, \hat{\tau}_3$ are the Pauli matrices in the spin and the particle-hole space, respectively. The in-plane (y - z) magnetizations of the neighboring F layers are not collinear in general, and form angles α_1 and α_2 with respect to the z -axis in the left (F_1) and the right (F_2) ferromagnets. The exchange field in ferromagnetic layers is $\mathbf{h}(x) = h_1(0, \sin \alpha_1, \cos \alpha_1)$ and $h_2(0, \sin \alpha_2, \cos \alpha_2)$.

We assume the superconductors are identical, with

$$\tilde{\Delta} = \begin{bmatrix} 0 & \hat{\sigma}_2 \Delta \\ \hat{\sigma}_2 \Delta^* & 0 \end{bmatrix} \quad (5)$$

for $x < -d_1$ and $x > d_2$. The self-consistency condition for the pair potential $\Delta = \Delta(x)$ is given by

$$\Delta = -i\lambda 2\pi N(0)k_B T \sum_{\omega_n} \langle f_{\uparrow\downarrow} \rangle, \quad (6)$$

where λ is the coupling constant, $N(0) = mk_F / 2\pi^2 \hbar^2$ is the density of states per spin projection at the Fermi level $E_F = \hbar^2 k_F^2 / 2m$, and $k_F = mv_F / \hbar$ is the Fermi wave number. In F layers $\tilde{\Delta} = 0$.

The supercurrent is obtained from the normal Green function through the following expression

$$I(\phi) = \pi e N(0) S k_B T \sum_{\omega_n} \sum_{\sigma} \langle v_x \text{Im } g_{\sigma\sigma} \rangle, \quad (7)$$

where ϕ is the macroscopic phase difference across the junction, and S is the area of the junction. In examples, the current is normalized to the resistance $R_N = 2\pi^2 \hbar / S e^2 k_F^2$.

Pair amplitudes, singlet f_s , and triplet f_{t0} and f_{t1} , with 0 and ± 1 projections of the total spin of a pair, are defined in terms of anomalous Green functions

$$f_s(x, t) = -i\pi N(0)k_B T \sum_{\omega_n} \langle f_{\uparrow\downarrow} - f_{\downarrow\uparrow} \rangle e^{-i\omega_n t}, \quad (8)$$

$$f_{t0}(x, t) = -i\pi N(0)k_B T \sum_{\omega_n} \langle f_{\uparrow\downarrow} + f_{\downarrow\uparrow} \rangle e^{-i\omega_n t}, \quad (9)$$

$$f_{t1}(x, t) = -i\pi N(0)k_B T \sum_{\omega_n} \langle f_{\uparrow\uparrow} + f_{\downarrow\downarrow} \rangle e^{-i\omega_n t}. \quad (10)$$

In the following we will characterize singlet amplitudes by the zero-time $f_s = f_s(x, 0)$. However, since zero-time triplet amplitudes identically vanish in agreement with the Pauli principle (with or without self-consistency),²⁵ we characterize triplets by auxiliary functions using summation over negative frequencies only,

$$f_{t0}^< = -i\pi N(0)k_B T \sum_{\omega_n < 0} \langle f_{\uparrow\downarrow} + f_{\downarrow\uparrow} \rangle, \quad (11)$$

$$f_{t1}^< = -i\pi N(0)k_B T \sum_{\omega_n < 0} \langle f_{\uparrow\uparrow} + f_{\downarrow\downarrow} \rangle. \quad (12)$$

Note that in previous definitions of triplet pair amplitudes the total spin of a pair is projected on the z -axis. Physically it is more reasonable to take directions of magnetizations in F layers as the spin quantization axes. New triplet amplitudes can be introduced in the F_1 layer ($-d_1 < x < 0$) by simple rotation

$$-i\tilde{f}_{t0} = \cos(\alpha_1)(-if_{t0}) - \sin(\alpha_1)f_{t1}, \quad (13)$$

$$\tilde{f}_{t1} = \sin(\alpha_1)(-if_{t0}) + \cos(\alpha_1)f_{t1}. \quad (14)$$

The same expressions with $\alpha_1 \rightarrow \alpha_2$ hold for F_2 layer, $0 \leq x < d_2$. Auxiliary functions $\tilde{f}_{t0}^<$ and $\tilde{f}_{t1}^<$ are related to $f_{t0}^<$ and $f_{t1}^<$ in the same way.

For $\phi = 0$, amplitudes f_s and $f_{t1}^<$ are real, while $f_{t0}^<$ is imaginary, and for $\phi = \pi$ the opposite is true. For $0 < \phi < \pi$, all amplitudes are complex. In the examples, we normalize the amplitudes to the value of f_s in the bulk superconductors,

$$f_{sb} = 2\pi N(0)k_B T \sum_{\omega_n} \frac{\Delta_0}{\sqrt{\omega_n^2 + \Delta_0^2}}. \quad (15)$$

Here, in the summation over ω_n , the high-frequency cutoff of $10\Delta_0$ is used. The temperature dependence of the bulk pair potential Δ_0 is given by $\Delta_0(T) = \Delta_0(0) \tanh(1.74\sqrt{T_c/T - 1})$.⁴⁵

We consider only transparent interfaces and use continuity of the Green functions as the boundary conditions. For planar $\text{SF}_1\text{F}_2\text{S}$ junctions (three dimensional case) Eq. (1) is solved iteratively together with the self-consistency condition, Eq. (6). The averaging over θ is given by $\langle \dots \rangle = (1/2) \int_0^\pi (\dots) d(\cos \theta)$.

Numerical computation is carried out using the collocation method. Iterations are performed until self-consistency is reached, starting from the stepwise approximation for the pair potential

$$\Delta = \Delta_0 \left[e^{-i\phi/2} \Theta(-x - d_1) + e^{i\phi/2} \Theta(x - d_2) \right], \quad (16)$$

where $\Theta(x)$ is the Heaviside step function. For finite electron mean free path in ferromagnets, the iterative procedure starts from the clean limit. We choose the appropriate boundary conditions in superconductors at the distance exceeding $2\xi_S$ from the SF interfaces. These boundary conditions are given by eliminating the unknown constants from the analytical solutions in stepwise approximation. To reach self-consistency starting from the stepwise Δ , five to ten iterative steps were sufficient for results shown in this article.

III. RESULTS

We illustrate our results on $\text{SF}_1\text{F}_2\text{S}$ planar junctions with relatively weak ferromagnets, $\hbar/E_F \sim 0.1$, and the ferromagnetic exchange length $\xi_F \sim 20k_F^{-1}$. Superconductors are characterized by the bulk pair potential at

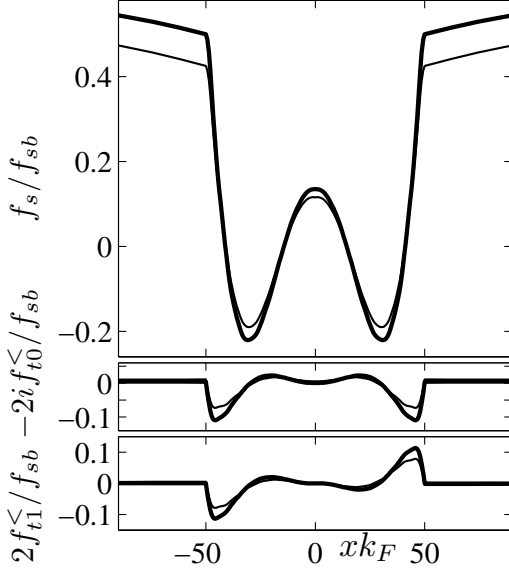


FIG. 2: Spatial dependence of singlet and triplet pair amplitudes f_s , $f_{t0}^<$, and $f_{t1}^<$, normalized to the bulk singlet amplitude f_{sb} . We consider a symmetric SF₁F₂S junction ($d_1 = d_2 = 50k_F^{-1}$) at low temperature, $T/T_c = 0.1$, with the electron mean free path in ferromagnets $l = 200k_F^{-1}$ (thick curves) and in the clean limit $l \rightarrow \infty$ (thin curves). The phase difference is $\phi = 0$. The magnetizations in ferromagnets are orthogonal, $\alpha_1 = -\pi/4$, $\alpha_2 = \pi/4$, and $h_1 = h_2 = 0.1E_F$. Superconductor is characterized by $\Delta_0(0)/E_F = 10^{-3}$.

zero temperature $\Delta_0(0)/E_F = 10^{-3}$, which corresponds to the superconducting coherence length $\xi_S(0) = 636k_F^{-1}$. We assume that all interfaces are fully transparent and the Fermi wave numbers in all metals are equal ($k_F^{-1} \sim 1\text{\AA}$).

Detailed analysis is given for symmetric junctions with relatively thin ($d_1 = d_2 = 50k_F^{-1}$) and thick ($d_1 = d_2 = 500k_F^{-1}$) ferromagnetic layers, Figs. 2–5, and for an highly asymmetric junction ($d_1 = 10k_F^{-1}$ and $d_2 = 990k_F^{-1}$), Figs. 6 and 7. In these examples $h_1 = h_2 = 0.1E_F$, $T/T_c = 0.1$, and both the clean limit ($l \rightarrow \infty$) and moderate disorder in ferromagnets ($l = 200k_F^{-1}$) are considered. The influences of temperature, thickness and exchange field variations are shown in Figs. 8 and 9 in the clean limit.

Short-ranged pair amplitudes f_s and $f_{t0}^<$ decay spatially from the FS interfaces in the same oscillatory manner. They decay algebraically with length $\hbar v_F/\hbar$ in the clean limit, and exponentially with the characteristic length $\sqrt{\hbar D/\hbar}$ in the dirty limit, where diffusion coefficient $D = v_F l/3$.

The long-ranged pair amplitude $f_{t1}^<$ is not suppressed by the exchange field and penetrates the ferromagnet on the scale $\hbar v_F/k_B T$ ($\sqrt{\hbar D/k_B T}$) in the clean (dirty) limit. In symmetric junctions ($d_1 = d_2$, $h_1 = h_2$, and $\alpha_1 = -\alpha/2$, $\alpha_2 = \alpha/2$) all pair amplitudes are practically the same in the clean limit ($l \rightarrow \infty$) and for moderate dis-

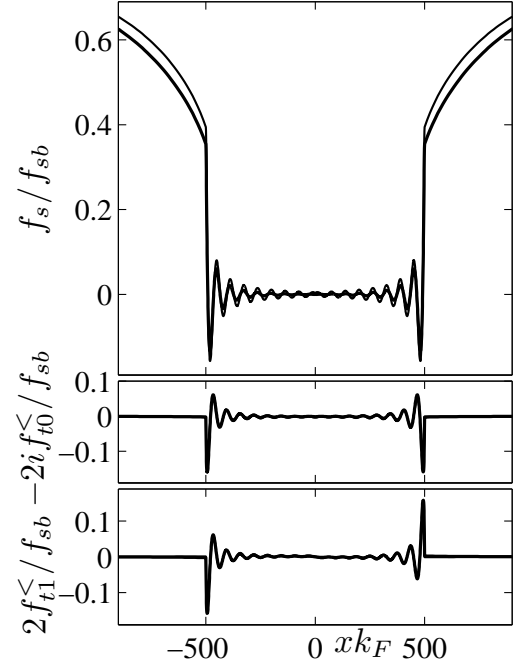


FIG. 3: The same as in Fig. 2 for ten times thicker ferromagnetic films, $d_1 = d_2 = 500k_F^{-1}$.

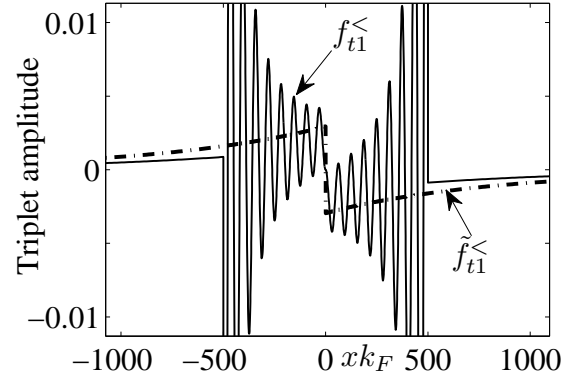


FIG. 4: Comparison between normalized triplet amplitudes $2f_{t1}^</f_{sb}$ (solid curve) and rotated $\tilde{f}_{t1}^</f_{sb}$ (dash-dotted curve). Parameters are the same as in Fig. 3 for $l \rightarrow \infty$.

order ($l = 200k_F^{-1}$) in ferromagnets, which is illustrated in Figs. 2 and 3. In symmetric junctions, $f_{t1}^<$ does not prevail; it can be seen in Fig. 5 that α -dependence of the Josephson critical current is monotonic.

Note that the spatial oscillations of $f_{t1}^<$ in Figs. 2–4 are due to our choice of z axis as the spin quantization axis. After choosing the magnetization in F layers as the spin quantization axis, the rotated amplitude $\tilde{f}_{t1}^<$ no longer oscillates but instead exhibits monotonic spatial variation with the jump at $x = 0$ (dash-dotted curve in Fig. 4). It can be seen that the amplitude $\tilde{f}_{t1}^<$ decays from F₁F₂ interface. This is because $\tilde{f}_{t1}^<$ in each F layer is generated at the interface itself by the projection $\tilde{f}_{t0}^< \sin \alpha$

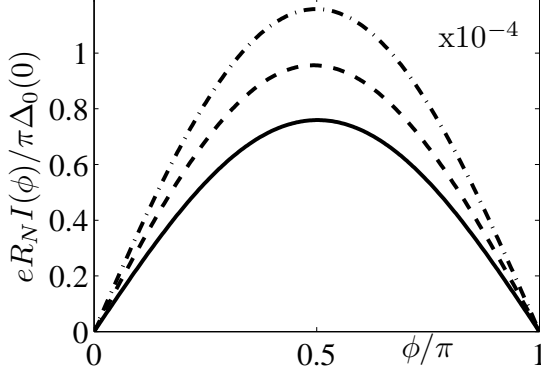


FIG. 5: The current-phase relation $I(\phi)$ for a symmetric SF_1F_2S junction with $d_1 = d_2 = 500k_F^{-1}$, $h_1 = h_2 = 0.1E_F$, $l = 200k_F^{-1}$, $T/T_c = 0.1$, and for three values of the relative angle between magnetizations: $\alpha = 0$ (solid curve), $\pi/2$ (dashed curve), and π (dash-dotted curve).

from the neighboring layer. The triplet pair amplitudes penetrate into superconductors and monotonically decay over the same distance (the bulk superconducting coherence length ξ_S) as the singlet amplitude saturates to the bulk value (see Fig. 4).

For thick F layers (when short-ranged amplitude $\tilde{f}_{t0}^<$ is highly suppressed at the F_1F_2 interface) the generated long-ranged component $\tilde{f}_{t1}^<$ is very small. Therefore, influence of misalignment of magnetizations on the Josephson current in symmetric SF_1F_1S junctions cannot be attributed to the emergence of spin-triplet correlations: For thin ferromagnetic layers all amplitudes are equally large, while for thick ferromagnetic layers the long range triplet \tilde{f}_{t1} is very small.

Fully developed long-range spin-triplet proximity effect emerges in asymmetric junctions with particularly thin and thick F layers (or weak and strong ferromagnets). The thin (weak) F layer acts as a “triplet-generator”, while the thick (strong) F layer is a “filter” which suppresses the short-ranged components. This is illustrated in Fig. 6 for thin F_1 layer ($d_1 = 10k_F^{-1}$) and thick F_2 layer ($d_2 = 990k_F^{-1}$) of equal strength $h_1 = h_2 = 0.1E_F$, with orthogonal magnetizations, $\alpha_1 = -\pi/2$ and $\alpha_2 = 0$. Here, magnetization in the thick (F_2) layer is taken along the z -axis and along the y -axis in the thin (F_1) layer. Because of this choice, the x -dependence of $f_{t1}^<$ is monotonic in F_2 . The thin layer thickness d_1 is chosen to give maximum triplet current for a moderate disorder in ferromagnets ($l = 200k_F^{-1}$). This explains why $f_{t1}^<$ in Fig. 6 is larger for the finite electron mean-free path than in the clean limit.

The current-phase relation for an highly asymmetric SF_1F_2S junction (the same parameters as in Fig. 6) is shown in Fig. 7. The critical current for orthogonal magnetizations is an order of magnitude larger than for collinear magnetizations even though the first harmonic is absent. The second harmonic is dominant like at 0-

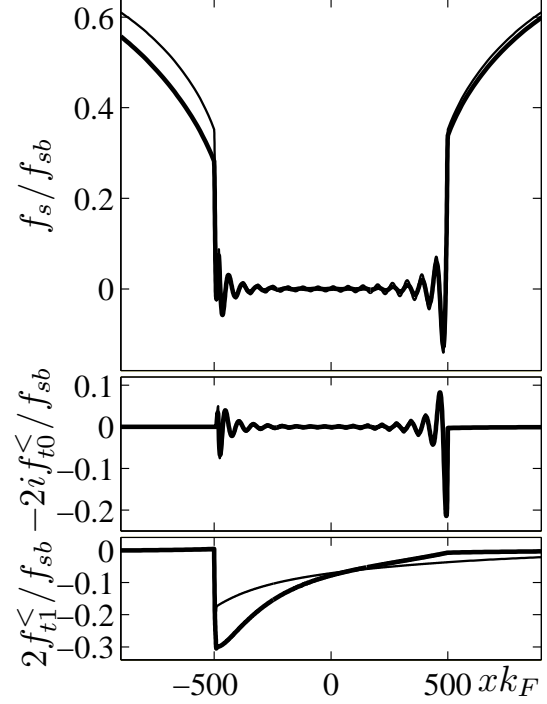


FIG. 6: Spatial dependence of singlet and triplet pair amplitudes f_s , $f_{t0}^<$, and $f_{t1}^<$, normalized to the bulk singlet amplitude f_{sb} . We consider an asymmetric SF_1F_2S junction ($d_1 = 10k_F^{-1}$ and $d_2 = 990k_F^{-1}$) at low temperature, $T/T_c = 0.1$, with the electron mean free path in ferromagnets $l = 200k_F^{-1}$ (thick curves) and in the clean limit $l \rightarrow \infty$ (thin curves). The phase difference is $\phi = 0$. Magnetization in the thin layer is along y -axis, $\alpha_1 = -\pi/2$, and along z -axis in the thick layer, $\alpha_2 = 0$. Here, $h_1 = h_2 = 0.1E_F$ and $\Delta_0(0)/E_F = 10^{-3}$.

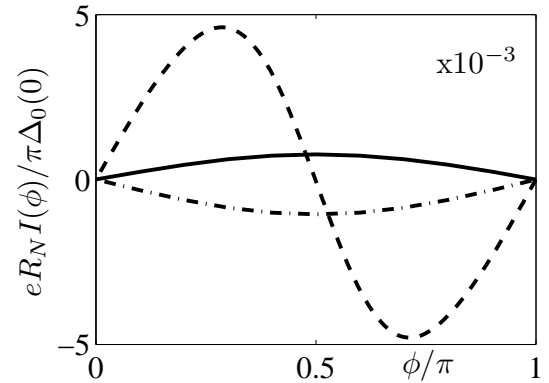


FIG. 7: The current-phase relation $I(\phi)$ for an asymmetric SF_1F_2S junction with $d_1 = 10k_F^{-1}$ and $d_2 = 990k_F^{-1}$, $h_1 = h_2 = 0.1E_F$, $l = 200k_F^{-1}$, $T/T_c = 0.1$, and for three values of the relative angle between magnetizations: $\alpha = 0$ (solid curve), $\pi/2$ (dashed curve), and π (dash-dotted curve).

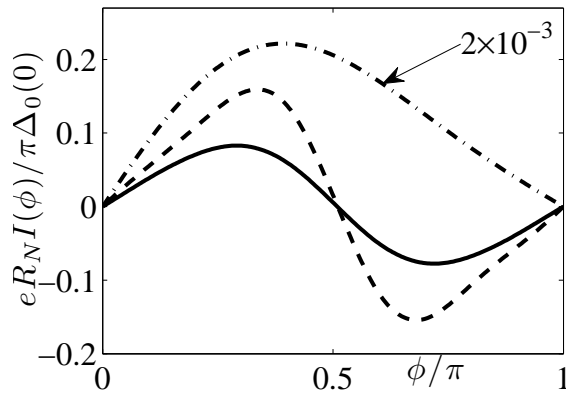


FIG. 8: The current-phase relation $I(\phi)$ for an asymmetric SF_1F_2S junction in the clean limit $l \rightarrow \infty$ with orthogonal magnetizations $\alpha = \pi/2$. For $d_1 = 10k_F^{-1}$, $d_2 = 990k_F^{-1}$, $h_1 = h_2 = 0.1E_F$ three cases are shown: $T = 0.1T_c$ (thick solid curve); $T = 0.01T_c$ (dashed curve); $T = 0.9T_c$ (dash-dotted curve, magnified 5×10^2 times).

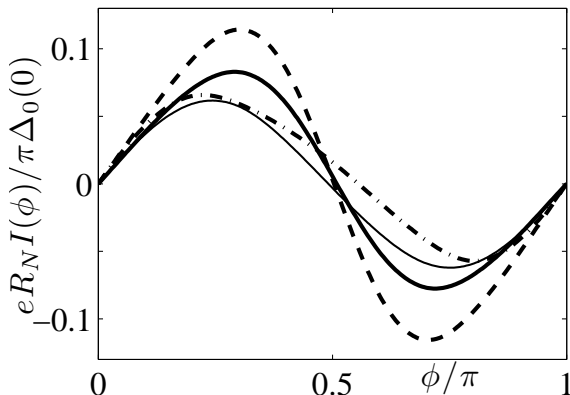


FIG. 9: The current-phase relation $I(\phi)$ for an asymmetric SF_1F_2S junction in the clean limit $l \rightarrow \infty$ with orthogonal magnetizations $\alpha = \pi/2$, and $T/T_c = 0.1$. For $d_1 = 10k_F^{-1}$, $d_2 = 990k_F^{-1}$, three cases are shown: $h_1 = h_2 = 0.1E_F$ (thick solid curve); $h_1 = 0.1E_F$, $h_2 = 0.2E_F$ (dashed curve); $h_1 = 0.05E_F$, $h_2 = 0.1E_F$ (dash-dotted curve). Influence of F layer thickness is shown for $d_1 = 20k_F^{-1}$, $d_2 = 980k_F^{-1}$, and $h_1 = h_2 = 0.1E_F$ (thin solid curve).

π transitions,^{37,46} except being larger in magnitude and long-ranged in the present case.

Robustness of the long-ranged second harmonic is illustrated in Figs. 8 and 9 in the clean limit. The magnitude of the second harmonic is enhanced by lowering the temperature, as can be seen from Fig. 8. This is in contrast to the temperature-induced $0-\pi$ transition in which the first harmonic is restored away from the transition temperature.⁴⁶⁻⁴⁸ When the temperature is close to the critical temperature T_c , the triplet proximity effect, i.e. the second harmonic in $I(\phi)$, is no longer dominant in an agreement with the results of Ref. 17. Small variations of the layers thickness and the exchange energy of

ferromagnets (Fig. 9), as well as moderate disorder (Fig. 7), do not affect the dominance of the long-ranged second harmonic at low temperatures. Since the influence of ferromagnet is determined by $\Theta = (h/E_F)k_F d$, the shown results remain the same for $\Theta_1 \sim 1$ in F_1 and $\Theta_2 \sim 100$ in F_2 layers.

In all calculations we have assumed transparent SF interfaces and clean or moderately disordered ferromagnets. Finite transparency much strongly suppresses higher harmonics than the first one and the considered effect becomes negligible in the tunnel limit. We expect the similar influence of large disorder: In diffusive SFS junctions at $0-\pi$ transition,^{47,48} where the second harmonic is dominant, the Josephson current drops to zero. However, this is not the case in the clean SFS junctions where the Josephson current is smaller but finite at the $0-\pi$ transition.⁴⁶

IV. CONCLUSION

We have studied the Josephson effect in SF_1F_2S planar junctions made of conventional superconductors and two monodomain ferromagnetic layers with arbitrary thickness, strength, and angle between in-plane magnetizations. We carried out a detailed analysis of spin-singlet and -triplet pairing correlations and the Josephson current in the clean limit and for moderate disorder in ferromagnets by solving self-consistently the Eilenberger equations. While the spin-singlet and -triplet correlations with zero spin projection are short range, the triplet correlations with a nonzero spin projection are long range and may have a dramatic impact on transport properties and the Josephson effect.

In symmetric SFFS junctions with ferromagnetic layers of equal strength, the long-range spin-triplet correlations have no substantial impact on the Josephson current both in the ballistic and moderately diffusive regimes: For thin (weak) ferromagnetic layers all amplitudes are equally large, while for thick (strong) layers the long-range triplet amplitude is very small. This explains the previous results of Refs. 23, 32.

We have found that fully developed long-range spin-triplet proximity effect occurs in highly asymmetric SF_1F_2S junctions at low temperatures and manifests itself as a dominant second harmonic in the Josephson current-phase relation. In contrast to the temperature-induced $0-\pi$ transition in which the first harmonic is restored away from the transition temperature, the magnitude of the second harmonic due to long-range spin-triplet correlations increases as the temperature is lowered. The triplet-induced second harmonic is robust against moderate disorder and variations in the layers thickness and exchange energy of ferromagnets.

Dominant second harmonic and the resulting ground state degeneracy of the Josephson junction (like at $0-\pi$ transitions) is experimentally accessible in asymmetric SF_1F_2S junctions with small interface roughness at low

temperatures. In addition, the half-periodicity of $I(\phi)$ in the considered junctions can be used for quantum interferometers (SQUIDs) which operate with two times smaller flux quantum and can exhibit the superposition of macroscopically distinct quantum states even in the absence of an external magnetic field.³⁷ This has a potential application in the field of quantum computing.⁴³

V. ACKNOWLEDGMENT

We acknowledge Mihajlo Vanević for help and for valuable discussions. The work was supported by the Serbian Ministry of Science, Project No. 171027.

-
- * Present address: Department of Physics, University of Basel, Klingelbergstrasse 82, CH-4056 Basel, Switzerland
- ¹ F. S. Bergeret, A. F. Volkov, and K. B. Efetov, *Rev. Mod. Phys.* **77**, 1321 (2005).
 - ² V. L. Berezinskii, *JETP Lett.* **20**, 287 (1974).
 - ³ F. S. Bergeret, A. F. Volkov, and K. B. Efetov, *Phys. Rev. Lett.* **86**, 4096 (2001).
 - ⁴ A. F. Volkov, F. S. Bergeret, and K. B. Efetov, *Phys. Rev. Lett.* **90**, 117006 (2003).
 - ⁵ I. Sosnin, H. Cho, V. T. Petrashov, and A. F. Volkov, *Phys. Rev. Lett.* **96**, 157002 (2006).
 - ⁶ R. S. Keizer, S. T. B. Goennenwein, T. M. Klapwijk, G. Miao, G. Xiao, and A. Gupta, *Nature* **439**, 825 (2006).
 - ⁷ M. S. Anwar, F. Czeschka, M. Hesselberth, M. Porcu, and J. Aarts, *Phys. Rev. B* **82**, 100501 (2010).
 - ⁸ J. Wang, M. Singh, M. Tian, N. Kumar, B. Liu, C. Shi, J. K. Jain, N. Samarth, T. E. Mallouk, and M. H. W. Chan, *Nature Phys.* **6**, 389 (2010).
 - ⁹ D. Sprungmann, K. Westerholt, H. Zabel, M. Weides, and H. Kohlstedt, *Phys. Rev. B* **82**, 060505(R) (2010).
 - ¹⁰ T. S. Khaire, M. A. Khasawneh, W. P. Pratt, and N. O. Birge, *Phys. Rev. Lett.* **104**, 137002 (2010).
 - ¹¹ J. W. A. Robinson, J. D. S. Witt, and M. G. Blamire, *Science* **329**, 59 (2010).
 - ¹² A. I. Buzdin, *Rev. Mod. Phys.* **77**, 935 (2005).
 - ¹³ M. L. Kulić and I. M. Kulić, *Phys. Rev. B* **63**, 104503 (2001).
 - ¹⁴ M. Eschrig, J. Kopu, J. C. Cuevas, and G. Schön, *Phys. Rev. Lett.* **90**, 137003 (2003).
 - ¹⁵ M. Eschrig and T. Löfwander, *Nature Phys.* **4**, 138 (2008).
 - ¹⁶ V. Braude and Y. V. Nazarov, *Phys. Rev. Lett.* **98**, 077003 (2007).
 - ¹⁷ M. Houzet and A. I. Buzdin, *Phys. Rev. B* **76**, 060504 (2007).
 - ¹⁸ A. F. Volkov and K. B. Efetov, *Phys. Rev. B* **78**, 024519 (2008).
 - ¹⁹ A. F. Volkov and K. B. Efetov, *Phys. Rev. B* **81**, 144522 (2010).
 - ²⁰ L. Trifunovic and Z. Radović, *Phys. Rev. B* **82**, 020505 (2010).
 - ²¹ M. Alidoust and J. Linder, *Phys. Rev. B* **82**, 224504 (2010).
 - ²² M. Duckheim and P. W. Brouwer, *Phys. Rev. B* **83**, 054513 (2011).
 - ²³ Z. Pajović, M. Božović, Z. Radović, J. Cayssol, and A. Buzdin, *Phys. Rev. B* **74**, 184509 (2006).
 - ²⁴ Y. Asano, Y. Tanaka, and A. A. Golubov, *Phys. Rev. Lett.* **98**, 107002 (2007).
 - ²⁵ K. Halterman, P. H. Barsic, and O. T. Valls, *Phys. Rev. Lett.* **99**, 127002 (2007).
 - ²⁶ K. Halterman, O. T. Valls, and P. H. Barsic, *Phys. Rev. B* **77**, 174511 (2008).
 - ²⁷ Y. Fominov, A. Golubov, and M. Kupriyanov, *JETP Lett.* **77**, 510 (2003).
 - ²⁸ C. You, Y. B. Bazaliy, J. Y. Gu, S. Oh, L. M. Litvak, and S. D. Bader, *Phys. Rev. B* **70**, 014505 (2004).
 - ²⁹ T. Löfwander, T. Champel, J. Durst, and M. Eschrig, *Phys. Rev. Lett.* **95**, 187003 (2005).
 - ³⁰ Y. S. Barash, I. V. Bobkova, and T. Kopp, *Phys. Rev. B* **66**, 140503 (2002).
 - ³¹ Y. V. Fominov, A. F. Volkov, and K. B. Efetov, *Phys. Rev. B* **75**, 104509 (2007).
 - ³² B. Crouzy, S. Tollis, and D. A. Ivanov, *Phys. Rev. B* **75**, 054503 (2007).
 - ³³ I. B. Sperstad, J. Linder, and A. Sudbø, *Phys. Rev. B* **78**, 104509 (2008).
 - ³⁴ T. Y. Karminskaya, A. A. Golubov, M. Y. Kupriyanov, and A. S. Sidorenko, *Phys. Rev. B* **79**, 214509 (2009).
 - ³⁵ Y. M. Blanter and F. W. J. Hekking, *Phys. Rev. B* **69**, 024525 (2004).
 - ³⁶ J. Linder, M. Zareyan, and A. Sudbø, *Phys. Rev. B* **79**, 064514 (2009).
 - ³⁷ Z. Radović, L. Dobrosavljević-Grujić, and B. Vujičić, *Phys. Rev. B* **63**, 214512 (2001).
 - ³⁸ H. Sellier, C. Baraduc, F. Lefloch, and R. Calemczuk, *Phys. Rev. Lett.* **92**, 257005 (2004).
 - ³⁹ J. R. Friedman, V. Patel, W. Chen, S. K. Tolpygo, and J. E. Lukens, *Nature* **406**, 43 (2000).
 - ⁴⁰ C. H. van der Wal, A. C. J. ter Haar, F. K. Wilhelm, R. N. Schouten, C. J. P. M. Harmans, T. P. Orlando, S. Lloyd, and J. E. Mooij, *Science* **290**, 773 (2000).
 - ⁴¹ A. Buzdin and A. E. Koshelev, *Phys. Rev. B* **67**, 220504 (2003).
 - ⁴² T. Yamashita, K. Tanikawa, S. Takahashi, and S. Maekawa, *Phys. Rev. Lett.* **95**, 097001 (2005).
 - ⁴³ T. P. Orlando, J. E. Mooij, L. Tian, C. H. van der Wal, L. S. Levitov, S. Lloyd, and J. J. Mazo, *Phys. Rev. B* **60**, 15398 (1999).
 - ⁴⁴ G. Eilenberger, *Z. Phys.* **190**, 142 (1966).
 - ⁴⁵ B. Mühlischlegel, *Z. Phys.* **155**, 313 (1959).
 - ⁴⁶ Z. Radović, N. Lazarides, and N. Flytzanis, *Phys. Rev. B* **68**, 014501 (2003).
 - ⁴⁷ V. V. Ryazanov, V. A. Oboznov, A. Y. Rusanov, A. V. Veretennikov, A. A. Golubov, and J. Aarts, *Phys. Rev. Lett.* **86**, 2427 (2001).
 - ⁴⁸ T. Kontos, M. Aprili, J. Lesueur, F. Genêt, B. Stephanidis, and R. Boursier, *Phys. Rev. Lett.* **89**, 137007 (2002).